

4. D. Branch and G. Tammann, *Annu. Rev. Astron. Astrophys.* **30**, 359 (1992).
5. M. M. Phillips, *Astrophys. J.* **413**, L105 (1993).
6. A. G. Riess, W. N. Press, R. P. Kirshner, *ibid.* **438**, L17 (1995); *ibid.* **473**, 88 (1996).
7. D. Branch, M. Livio, L. R. Yungelson, F. R. Boffi, E. Baron, *Publ. Astron. Soc. Pac.* **107**, 717 (1995); A. Renzini, in *IAU Colloquium 145, Supernovae and Supernova Remnants*, R. McCray and Z. Wang, Eds. (Cambridge Univ. Press, Cambridge, 1996), pp. 77–85.
8. I. Iben Jr. and A. Tutukov, *Astrophys. J. Suppl. Ser.* **55**, 335 (1984); R. Webbink, *Astrophys. J.* **277**, 355 (1984).
9. For example, K. Nomoto, *Astrophys. J.* **253**, 798 (1982); _____ and Y. Kondo, *ibid.* **367**, L19 (1991); K. Nomoto *et al.*, in *Supernovae* (Les Houches, Session LIV), S. Bludman *et al.*, Eds. (Elsevier Science, Amsterdam, 1994), pp. 199–249.
10. I. Hachisu, M. Kato, K. Nomoto, *Astrophys. J.* **470**, L97 (1996).
11. K. Nomoto, *ibid.* **257**, 780 (1982); M. Hashimoto, K. Nomoto, K. Arai, K. Kaminisi, *ibid.* **307**, 687 (1986).
12. S. E. Woosley and T. A. Weaver, *ibid.* **423**, 371 (1994).
13. E. P. J. van den Heuvel, D. Bhattacharya, K. Nomoto, S. A. Rappaport, *Astron. Astrophys.* **262**, 97 (1992); S. A. Rappaport, R. DiStefano, J. Smith, *Astrophys. J.* **426**, 692 (1994).
14. P. Ruiz-Lapuente *et al.*, *Nature* **365**, 728 (1993).
15. W. D. Arnett, *Nucleosynthesis and Supernovae* (Princeton Univ. Press, Princeton, NJ, 1996); S. E. Woosley, in *Supernovae*, A. Petschek, Ed. (Springer, New York, 1990), pp. 182–212.
16. Fe peak elements consist of mostly Fe and Ni with some Ti, V, Cr, Mn, and Co.
17. For example, J. Niemeyer and W. Hillebrandt, *Astrophys. J.* **452**, 769 (1995); J. Niemeyer and S. E. Woosley, *ibid.* **475**, 740 (1997).
18. K. Nomoto, F.-K. Thielemann, K. Yokoi, *ibid.* **286**, 644 (1984); F.-K. Thielemann, K. Nomoto, K. Yokoi, *Astron. Astrophys.* **158**, 17 (1986); H. Yamaoka, T. Shigeyama, K. Nomoto, F.-K. Thielemann, *Astrophys. J.* **393**, L55 (1992).
19. A. M. Khokhlov, *Astron. Astrophys.* **245**, 114 (1991); S. E. Woosley and T. A. Weaver, in *Supernovae* (Les Houches, Session LIV), S. Bludman *et al.*, Eds. (Elsevier Science, Amsterdam, 1994), pp. 63–154.
20. A. M. Khokhlov, *Astron. Astrophys.* **245**, L25 (1991); W. D. Arnett and E. Livne, *Astrophys. J.* **427**, 314 (1994).
21. E. Livne, *Astrophys. J.* **354**, L53 (1990).
22. T. Shigeyama, K. Nomoto, H. Yamaoka, F.-K. Thielemann, *ibid.* **386**, L13 (1992); J. C. Wheeler and R. Harkness, *Rep. Prog. Phys.* **53**, 1467 (1990).
23. P. Nugent, E. Baron, D. Branch, A. Fisher, P. Hauschildt, *Astrophys. J.*, in press.
24. P. Höflich and A. Khokhlov, *ibid.* **457**, 500 (1996).
25. For example, P. Mazzali, I. J. Danziger, M. Turatto, *Astron. Astrophys.* **297**, 509 (1995); M. Turatto *et al.*, *Mon. Not. R. Astron. Soc.* **283**, 1 (1997).
26. P. Nugent, E. Baron, D. Branch, *Astrophys. J.* **455**, L147 (1995).
27. For example, D. Jeffery *et al.*, *ibid.* **397**, 304 (1992); A. Fisher, D. Branch, P. Höflich, A. Khokhlov, *ibid.* **447**, L73 (1995); W. P. S. Meikle *et al.*, *Mon. Not. R. Astron. Soc.* **281**, 263 (1996).
28. P. Höflich *et al.*, *Astrophys. J.* **472**, L81 (1996).
29. M. Hashimoto, K. Nomoto, F.-K. Thielemann, *Astron. Astrophys.* **210**, L5 (1989); F.-K. Thielemann, K. Nomoto, M. Hashimoto, *Astrophys. J.* **460**, 408 (1996); T. Tsujimoto *et al.*, *Mon. Not. R. Astron. Soc.* **277**, 945 (1995); see also S. E. Woosley and T. A. Weaver, *Astrophys. J. Suppl. Ser.* **101**, 181 (1995).
30. K. Nomoto *et al.*, in (3), pp. 349–378.
31. S. van den Bergh and G. A. Tammann, *Annu. Rev. Astron. Astrophys.* **29**, 363 (1991).
32. For example, Y. Yoshii, T. Tsujimoto, K. Nomoto, *Astrophys. J.* **462**, 266 (1996).
33. M. Hamuy *et al.*, *Astron. J.* **109**, 1 (1995); *ibid.* **112**, 2398 (1996).
34. A. Sandage *et al.*, *Astrophys. J.* **460**, L15 (1996); A. Saha *et al.*, *ibid.*, in press.
35. B. E. Schaefer, *ibid.* **460**, L19 (1996).
36. W. D. Arnett, D. Branch, J. C. Wheeler, *Nature* **314**, 337 (1985).
37. D. Branch, P. Nugent, A. Fisher, in (3), pp. 715–734.
38. P. Ruiz-Lapuente, *Astrophys. J.* **465**, L83 (1996).
39. The Supernova Cosmology Project: S. Perlmutter *et al.*, *ibid.*, in press; *IAU Circular* 6596 (1997).
40. The High-Z Supernova Search Team: B. Schmidt *et al.*, *IAU Circular* 6602 (1997).
41. P. Ruiz-Lapuente, A. Burkert, R. Canal, *Astrophys. J.* **447**, L69 (1995); R. Canal, P. Ruiz-Lapuente, A. Burkert, *ibid.* **456**, L101 (1996).
42. Supported in part by a grant-in-aid for scientific research (05242102, 06233101, 4227) and COE research (07CE2002) of the Ministry of Education, Science, and Culture of Japan.

Planetary Nebulae: Understanding the Physical and Chemical Evolution of Dying Stars

Ronald Weinberger and Florian Kerber

Planetary nebulae are one of the few classes of celestial objects that are active in every part of the electromagnetic spectrum. These fluorescing and often dusty expanding gaseous envelopes were recently found to be quite complex in their dynamics and morphology, but refined theoretical models can account for these discoveries. Great progress was also made in understanding the mechanisms that shape the nebulae and the spectra of their central stars. In addition, applications for planetary nebulae have been worked out; for example, they have been used as standard candles for long-range distances and as tracers of the enigmatic dark matter.

Planetary nebulae (PNe) were so called because their often faint disks resembled images of Uranus and Neptune. The oldest known discovery of a PN dates back to Messier, who in 1784 catalogued the Dumbbell nebula, NGC 6853, as Messier 27 (1). Actually, PNe are gaseous nebulae, although they often contain a great deal of dust, and originate as envelopes thrown off from stars in advanced evolutionary stages. Starting as dense, compact objects, they brighten as they expand and fluoresce with radiation absorbed in the ultraviolet (UV) spectral range as the condensed core of the dying star attains a high surface temperature ($\geq 30,000$ K) and radiates copiously at wavelengths less than 91.2 nm. Eventually, as the density of the expanding envelope drops, the surface brightness falls abruptly, and the nebulae disappear. The ejected material returns to the interstellar medium (ISM). The remnant stars, called central stars (CSs) because of their location in or near the centers of the PNe, become white dwarf stars during the latest phases of the evolution of the nebulae.

Planetary nebulae are found not only in our galaxy, but also in other galaxies. About one to two times every year, a star of mass ≤ 1 solar mass (M_{\odot}) is born in our Milky Way. Almost 99% of all stars are less massive than $10 M_{\odot}$, and those with masses of 1 to $8 M_{\odot}$ will almost certainly go through the PN phase, provided they are single stars or

are in a wide binary (2). On the other hand, it has long been established that white dwarfs have a narrow range of masses sharply peaking around $0.6 M_{\odot}$ (3). Consequently, in several cases, considerable mass is lost to the ISM, and a part of this mass, up to $1 M_{\odot}$ per PN, is in the form of these nebulae, which usually expand with velocities of about 20 to 30 km s^{-1} .

Study of PNe and their CSs provides understanding about the chemical and physical evolution of the majority of stars. By comparing observations with theoretical models of star evolution, it was possible to understand why and how PNe form, how the nebulae and the CSs develop, and how the internal structure and chemical composition of the CS are reflected in the physical conditions of the PN (4). Astronomers also study PNe to learn about the chemical evolution of galaxies. The abundances of various elements in PNe trace the abundances of the ISM, from which the progenitor stars originally formed, and the surface abundances of the immediate precursor stars of PNe, which were enriched by material dredged up to their surfaces from interior regions of nucleosynthesis. Thus, by studying chemical abundances in PNe, astronomers are able to trace the history of galactic chemical evolution and help constrain models of stellar evolution. The abundances of the elements N, C, and He are the result of stellar nucleosynthesis, whereas O, Ne, Ar, and S trace the metallicity of the region in which the star formed (5).

Planetary nebulae are also useful yard-

The authors are at the Institut für Astronomie der Universität Innsbruck, Technikerstrasse 25/8, A-6020 Innsbruck, Austria.

sticks for measuring the distance and age of nearby regions of the universe: Although distances of individual local PNe are hard to determine, these PNe still serve as some of the most useful of the standard candles for determining the distances of galaxies more remote than about 30 million light years. The PNe luminosity function is remarkably stable from galaxy to galaxy; with special filters to isolate emission lines like the [O III] lines (6), a number of PNe can be measured in a galaxy, and a luminosity function can be constructed and compared with that of a nearby galaxy of well-known distance, such as the Andromeda Galaxy (7).

Origin of Planetary Nebulae

Over the past three decades, a highly stylized picture has been painted of how the vast majority of stars become asymptotic giant branch (AGB) stars and how they subsequently develop into PNe (8). The AGB phase of evolution is preceded by the main sequence (core H-burning) phase and the core He-burning phase. The pace of evolution depends on the mass and chemical composition: The time spent on the main sequence is $\approx 10^{10}$ years for a $1 M_{\odot}$ star and $\approx 10^8$ years for a $5 M_{\odot}$ star. According to the models, such stars become AGB stars, although their tracks look quite different (Fig. 1). After the red-giant branch (RGB), they evolve upward along the AGB. In the early AGB phases, He burns in a shell; then H is re-ignited, burning in a shell above the He shell, and the star thereafter alternately burns H and He in shells above an electron-degenerate C, O, and Ne core. This phase is the important thermally pulsating AGB stage. Convective mixing causes the abundance of C, N, and O in the envelope to increase, and the simultaneous increase in opacity leads to an expansion of the envelope. Acoustical oscillations develop shocks, which cause the atmosphere to expand, and radiation pressure on freshly formed dust grains leads to a stellar wind that grows in strength. As the AGB star brightens, the rate of mass loss from its surface accelerates, and eventually there is a complete detachment of an expanding, ejected shell from a contracting stellar remnant. Once the mass of the H-rich matter left in the envelope decreases below a certain critical value, the remnant star leaves the AGB and rapidly evolves to the high-temperature part of the Hertzsprung-Russell (HR) diagram. When the surface of the star becomes hot enough, photons from the remnant cause a portion of the expelled nebula to fluoresce at optical wavelengths. A PN has been born; it will be further shaped by fast gas particles from the CS and can be observed at optical,

infrared, and radio wavelengths. Evolutionary models show that a $1 M_{\odot}$ star will result in a CS of $0.6 M_{\odot}$ —that is, the mass lost since departure from the main sequence will amount to $0.4 M_{\odot}$ —whereas a $5 M_{\odot}$ star will lose considerably more mass—more than $4 M_{\odot}$ will be blown off, and a mere $0.85 M_{\odot}$ will remain.

The mechanism of mass loss together with subsequent shaping processes lead to a multitude of PNe morphologies. A detailed examination of PNe morphology carried out almost eight decades ago resulted in the classifications helical, annular, disk, amorphous, and stellar (9). Subsequent schemes frequently used similar descriptive forms: elliptical, rings, bipolar, round, or butterfly. A considerable fraction of PNe have multiple envelopes; that is, they consist of an inner envelope showing some specific morphology surrounded by an often round shell, called the halo. The two most common morphologies are a double-peaked structure along the minor axis with extended emission along the major axis, often referred to as bipolar, and elliptical structures, both showing a wealth of various features (Fig. 2).

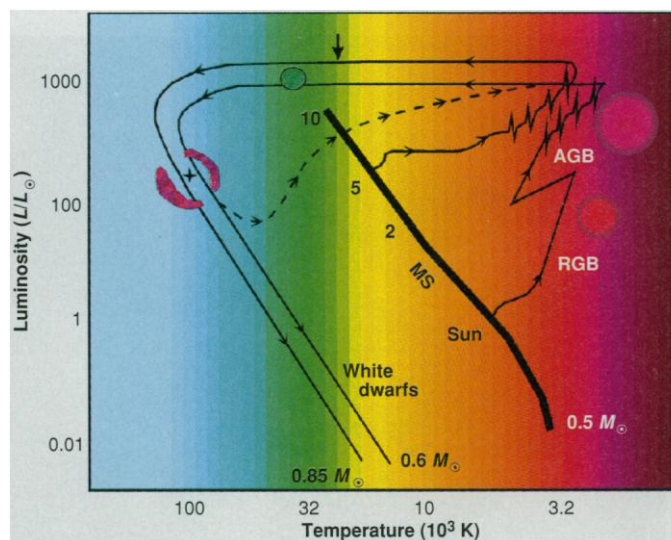
The origin of such diverse shapes has remained a mystery for a long time. Binary CSs could have major effects on the nebular shapes: A common envelope of gas and dust around these stars may form, and the early mass ejection would probably be spherically

symmetric. At later times, a thick disk would form around the binary, and mass would be preferentially ejected in the orbital plane of the binary, leading to a large contrast in density between the equatorial and polar directions of the resulting PN (10). However, the widely observed asymmetries seen in the shapes of PNe do not necessarily imply binary CSs: The effects of a slow stellar rotation of a single AGB star can lead to mass loss predominantly in the equatorial plane of the star, thus also favoring a bipolar morphology (11). Generally, it is believed that the morphology and expansion of PNe are the result of an interaction between a fast CS wind with the remnant circumstellar envelope of the AGB progenitor (12). A prediction of the interacting-winds theory is being investigated by the x-ray-sensitive Röntgen Satellite (ROSAT) (13). Shock waves generated by the interacting winds are believed to generate a hot bubble inside of the PN. With a temperature of a few millions of kelvin, this bubble radiates x-rays. The initial results show that ROSAT indeed detected several PNe.

Planetary Nebula Physics

A fully formed PN will not appear until the surface of the CS heats to about 30,000 K. At this temperature, the star will emit UV photons with energies of about 10 to 100

Fig. 1. Hertzsprung-Russell (HR) diagram, which plots the surface temperature of a star versus its luminosity L (L_{\odot} is the luminosity of the sun). About 90% of all stars in the Milky Way lie on a single narrow band diagonally from hot, bright stars to faint, cool ones: This region is known as the main sequence (MS), numbers indicate star masses in units of M_{\odot} . Giants and supergiants are much more luminous at a given color, at the cool end of the diagram. Well below the main sequence are the white dwarfs. The position of a star in the HR diagram is mainly determined by two parameters, mass and age (by age, the stage of evolution is meant; different stars evolve at different rates and therefore reach similar stages of evolution with different ages in years). In recent years, the HR diagram and variations of it are mainly used for comparison of sophisticated theoretical stellar models with observations. The two solid lines are evolutionary tracks (arrows show direction of evolution) of stars that leave the main sequence at 1 and $5 M_{\odot}$ and end as white dwarfs of 0.6 and $0.85 M_{\odot}$, respectively. Between the thick vertical arrow that marks the onset of photo-ionization and the white dwarf regime, these stars are the central stars of their PNe. RGB means red giant branch, and AGB means asymptotic giant branch. Spikes in the diagram represent thermal pulses, and the dashed line represents a "born-again" evolution.



eV. These energetic photons will ionize the surrounding gas, which will then emit its own light. The bulk of such a gaseous envelope is ionized H and He, but the minor constituents—heavier elements like N, O, and S—also show up prominently in an optical spectrum as emission lines (Fig. 3); in bright nebulae, many more elements can be detected (14). Emission lines are the result of transitions between different electronic states of the ion, and the upper levels of these transitions can be populated by electrons that either recombined to that state or were promoted from lower levels as a result of energetic collisions. With the use of diagnostic emission-line ratios, physical properties of the nebulae can be deduced. Typical values for the electron temperature derived from the [O III] lines are 10^4 K, and typical electron densities, for example, from the [S II] doublet give a range from 10^2 to 10^4 cm^{-3} (15).

The hot CSs emit most of their radiation in the UV region. Photons with wavelengths shorter than 91.2 nm ionize H from its ground state (energy $E \geq 13.6$ eV). This photo-ionization process is responsible for the existence of the H envelope and the strong recombination lines of H and He. Thus, a PN is not in thermodynamic equilibrium: The observed gas is fully ionized but is in a low state of excitation at the same time. Two cases in point are “forbidden” line emission (6) and two-photon emission. The extremely low particle densities in the PNe

plasma allow forbidden emission from the heavier elements (such as N, O, and S), despite the long lifetimes, seconds or even hours, of the collisionally populated metastable states from which they originate (16).

About 20,000 years after the red giant expels its outer envelope, the wind is still fast, but the mass loss has decreased to about $10^{-8} M_{\odot} \text{ year}^{-1}$. When the hot bubble reaches the outer borders of the slow wind material, it is no longer confined and may break out into the ISM. Because the physical circumstances, such as wind velocities and degree of density contrast in the envelope, vary from object to object, the development of the dynamics, of density and temperature, is different among PNe. Consequently, the morphology is, as a rule, complex even on small scales and acts as a tracer of the physical conditions in the PN. To this end, the images of PNe taken with the Hubble Space Telescope (HST) are of considerable help, because they show a wealth of morphological features, the physical details of which are in the process of being studied (Fig. 2).

After a few tens of thousands of years, the winds stop, and the PN fades as the ejected gases mix with the ISM. Evolved PNe may interact with the surrounding ISM. The morphologies that were originally produced by the initial ejection processes and subsequent shaping processes fade and become less detectable in most cases, allowing the PN-ISM interaction to emerge as the domi-

nant process. In physical terms, the density decreases as the PN ages; at a critical point, the ISM pressure upstream becomes comparable to the pressure in the PN shell, and the gas in the envelope is compressed. The consequent increase in density results in a higher recombination rate, which in turn leads to a lower degree of ionization and an asymmetric brightness distribution. Therefore, the brightness enhancement is most prominent in the lines of low ionization stages like [N II] and [O I]. Over time, the density drops further, and upon reaching a certain low density (typically a few electrons per cubic centimeter), the expansion of the PN is significantly slowed upstream, leading to a deformation of the nebula (17). At first its shape may turn into a blunt parabola, but complicated motions in the interaction zone may lead to a severe distortion. During this process, the CS, which is not affected by the slowing, moves out of the geometrical center of the PN, carrying its own sphere of ionized H with it, provided it is still hot enough. This scenario has been observed in Sh 2-174 (18). The final result of this evolution is a white dwarf stripped of its nebula, which mixes with the ISM, returning to it processed material that was dredged up from the interior of the CS in earlier phases.

Central Stars

The majority of PNe have a fairly faint CS with a low apparent optical brightness, from about 10th magnitude to values beyond the

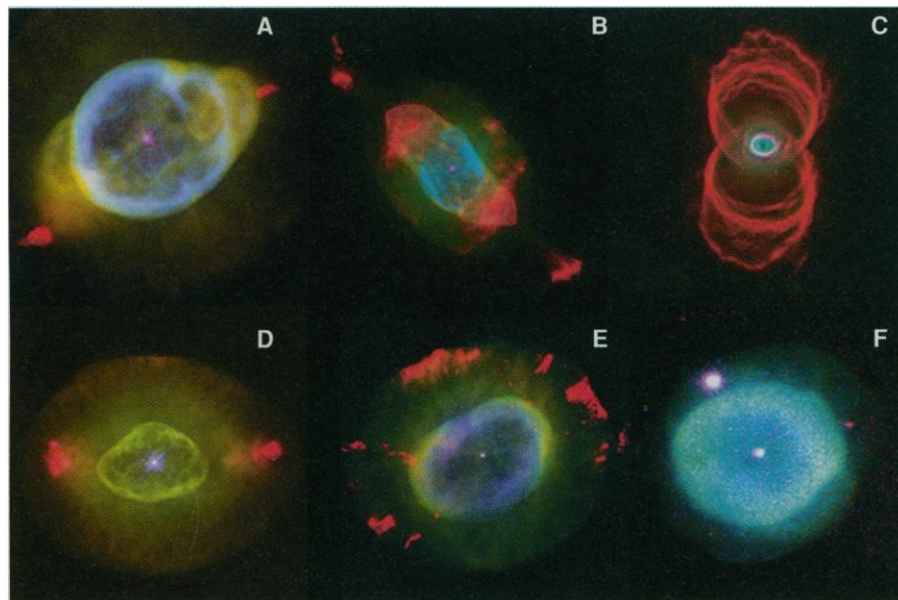


Fig. 2. A mosaic of six PNe (38) showing the diversity of morphological details found in these objects. The images are composite illustrations, with N emission in red, H emission in green, and O emission in blue. The CSs can be seen as small dots at the centers of the nebulae. (A) NGC 3242 is of bipolar type, whereas (B) NGC 7009, (C) MyCn 18, (D) NGC 6826, (E) NGC 7662, and (F) NGC 2610 are elliptical nebulae, showing various degrees of ellipticity. Note the presence of halos in all objects except NGC 7009 and MyCn 18. The image of NGC 2610 was taken with the 2.1-m telescope of Kitt Peak National Observatory, and all others were taken with the HST.

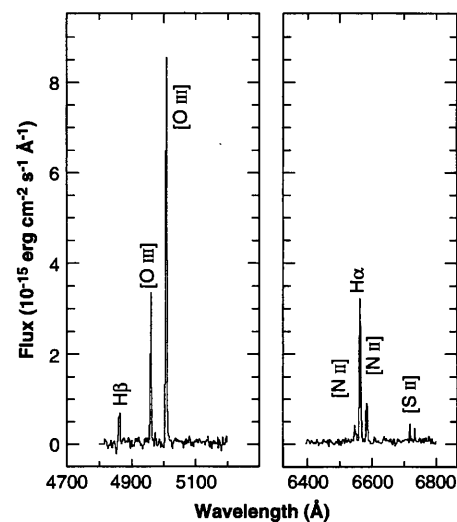


Fig. 3. Optical spectrum of the faint PN G257.8-5.4 (6). This spectrum is typical in the sense that the vast majority of known PNe are of low surface brightness, where the spectrum is not rich in lines (there was no signal above noise at wavelengths between those shown in the panels). In the case of bright, young PNe, one could expect many strong emission lines in the UV and optical wavelength ranges and dust features in the infrared.

limits of visibility with the largest telescopes. Thus, none of the CSs is visible with the unaided eye. Several CSs are members of a binary system: The primary goal of an ongoing snapshot survey by the HST is to identify resolved visual-binary companions of CSs, in order to determine accurately distances to PNe by means of main-sequence fitting. Over a dozen companions have been detected so far (19). Of the fundamental data, the brightness is particularly important, because it is used for temperature and luminosity determinations. A problem for accurate measurements is the PN background, which frequently distorts and falsifies measurements (20). The most outstanding characteristics of CSs are that they are hot, with surface temperatures ranging from 30,000 to 300,000 K, and the high energy density in the radiation fields of such hot stars produces two major difficulties for theoretical modeling: strong stellar winds and departures from local thermal equilibrium in the photosphere.

Central stars copiously emit UV radiation. Progress was made in the field of temperature determinations and wind characteristics by the International Ultraviolet Explorer (IUE) satellite. However, as to temperature determinations, the IUE could not observe stars fainter than magnitude of about $m_V \approx 18$, limiting the number of CSs that could be observed. An independent method in the optical regime proved to be useful: For CSs that are bright enough to allow the acquisition of high-resolution absorption line profiles, brighter than $m_V \approx 18$, it was possible to derive both the surface temperature and the surface gravity by analyzing the line profiles in terms of model atmospheres (21). Recent results give much more accurate determinations of the CS temperatures when compared to earlier efforts.

The information on wind characteristics and mass loss of the CSs comes essentially from P Cygni profiles (22) of resonance or excited lines of heavy ions like C, O, and N observed in the UV by the IUE. To derive the mass loss rate, one can distinguish between “theoretical” and “semi-empirical” methods. In both cases, the calculated P Cygni profiles must match the observed ones. In the first type, the mechanisms responsible for the production of the wind are theoretically specified, whereas in the semi-empirical methods, the velocity law is assumed and is used as a parameter to fit the observations. The mass loss rates observed are in the range of 10^{-6} to $10^{-11} M_{\odot} \text{ year}^{-1}$ (23).

Because CSs end as white dwarfs and because very extended (that is, old) PNe of low surface brightness can best be observed at optical wavelengths, a large amount of

theoretical and observational work has been devoted to these pre-white dwarf stars during the last decade (24). Among them, the PG 1159 stars are H-deficient objects that have long defied a quantitative spectroscopic analysis because of their extremely high temperatures and peculiar surface composition. Their atmospheres are mainly composed of He, C, and O, suggestive of deep intershell matter that has gone through the triple- α -burning phase and has been dredged up to the surface (25). The “born-again” scenario appears to be the most plausible explanation for this conspicuous behavior (26): Under appropriate conditions, heating of the He layer above the core may lead to a He-burning runaway, the consequences of which are to carry the star back to the AGB; subsequently, the star retraces its evolutionary steps as a H burner and evolves into a white dwarf again (Fig. 1). For these objects, the characteristics of the CS and the surrounding PN may change on time scales short enough to be witnessed over a few observing seasons.

It seems that such a discovery was made last year. Initially classified as a slow nova (27), this star, “Sakurai’s object,” seems to be undergoing a late He-shell flash. The first PN has subsequently been found, and a spectrum reveals it to be an ordinary PN. The spectrum of the CS is reminiscent of an F-type supergiant but has additional lines of C, N, and O; observed changes in the spectrum within 1 year—the emerging of C_2 Swan bands and the weakening of the H lines—are much faster than anticipated from theory and are a challenge for the interpretation (28). A late He flash is a rare event to observe: The last one on record is V 605 Aql in 1919 (29). Another candidate is FG Sge, which has experienced dramatic development throughout the HR diagram over the last 100 years (30). The H-deficient inner nebulae of a tiny group of additional PNe (A 30, A 78) were probably created by this process thousands of years ago (31).

Other Applications for PNe

Great emphasis has been placed on PNe in the Magellanic clouds and other nearby galaxies. One gives up spatial resolution and accepts small fluxes in studying these PNe but gains the advantage of dealing with a sample at a known distance, thus avoiding the worst problem in galactic PNe research, the distance problem. Luminosity functions of PNe outside of the Milky Way contain information about CS mass distributions; nebular, CS, and progenitor evolution; stellar death rates; and a galaxy’s star-formation and chemical-evolution histories. The increased awareness derives mainly from use

of the luminosity function of the [O III] line at 500.7 nm to derive distances to galaxies. These distances have significant consequences for the Hubble constant and the age of the universe (32). For example, an [O III] survey for PNe has recently been completed in the giant spiral galaxy M101. From these PNe data and the empirical PN luminosity function, a distance to M101 has been derived that is in excellent agreement with the distance determined from HST observations of Cepheids. This observation demonstrates that the luminosity function technique can be successfully applied to spiral galaxies and is a powerful, independent method with which to determine the Hubble constant (33).

Planetary nebulae are valuable tracers of dark matter in galaxies. Because PNe exist not only in a galaxy’s plane but also in its halo, their orbital motions are affected by normal luminous matter as well as by the invisible dark matter in the halo. For example, spectroscopic observations of PNe with the New Technology Telescope of the European Southern Observatory have achieved important results for understanding the dark matter content and the formation mechanism of the giant elliptical galaxy NGC 1399: Thirty-seven PNe were found to be moving so quickly that they would fly off into intergalactic space if NGC 1399 does not contain about 10 times more mass than one can infer from just the stars and bright gas (34). This discovery fortifies the growing evidence that the universe consists largely of invisible dark matter, which continues to elude detection or easy explanation.

About two decades ago, it came as a surprise that PNe, with their plasma temperature of $\approx 10,000$ K, contain dust; about one decade ago, observations revealed that many PNe are surrounded by envelopes of neutral gas where molecules—for example, CO—and neutral H exist and whose mass often exceeds that of the ionized nebulae (35). Dust and neutral gas have been thoroughly studied by means of ground-based infrared instrumentation, the Infrared Astronomical Satellite (IRAS), the Infrared Space Observatory (ISO), and radio and millimeter-wavelength telescopes. The mere coexistence of hot gas and cold (less than a few hundred kelvin) gas or dust is a challenge for nebular models; similar phenomena exist in other types of nebulae, for example, in H II regions and some supernova remnants. The solution to this puzzle, probably valid also for other types of emission nebulae, is the pronounced inhomogeneity of the nebulae: They are clumped on the smallest size scales observed. An extreme form of such inhomogeneity is seen in the numerous clumps inside the ionized cavity of the Helix nebula,

where the optical condensations are ≈ 1 arc sec in size (36); their masses are about $10^{-5} M_{\odot}$ or less per clump, and their number may total 3500. In all probability, their mass loss is very low, thus allowing a lifetime exceeding that of the PN stage. At present, it is not known what the fate of these clumps is, if they survive. If they are gravitationally bound, they will eventually collapse into solid bodies, leaving behind a cooling white dwarf surrounded by thousands of planets; otherwise, they will expand and dissipate once the PN stage has transpired.

REFERENCES AND NOTES

1. C. Messier, list of nebulous objects, originally published in *Connaiss. Temps* (1784); republished by H. Shapley and H. Davis, *Observatory* **41**, 318 (1918).
2. Wide binaries are noninteracting double stars, that is, there is or was no mass exchange or mass overflow from one component to the other, in contrast to close binaries, for which, in the case of mass loss by one component, a "common envelope" may form.
3. V. Weidemann, *Annu. Rev. Astron. Astrophys.* **28**, 103 (1990).
4. S. Kwok, *Publ. Astron. Soc. Pac.* **106**, 344 (1994).
5. R. L. Kingsburgh and M. J. Barlow, *Mon. Not. R. Astron. Soc.* **271**, 257 (1994).
6. Expressions like [O III] indicate emission lines. For example, O III indicates doubly ionized oxygen (a I implies neutral gas). Brackets indicate a "forbidden" transition, which are hardly or not at all observable under normal laboratory conditions because of the extremely low plasma densities from which they originate.
7. G. Jacoby, L. Ciardullo, H. Ford, *Astrophys. J.* **356**, 332 (1990).
8. The asymptotic giant branch (AGB) is so called because the calculated evolutionary tracks approach the giant branch more or less asymptotically. I. Iben Jr., *Phys. Rep.* **250**, 1 (1995).
9. H. D. Curtis, *Publ. Lick Obs.* **13**, 55 (1918).
10. F. A. Rasio and M. Livio, *Astrophys. J.* **471**, 366 (1996).
11. E. A. Dorfi and S. Höfner, *Astron. Astrophys.* **313**, 605 (1996).
12. G. Mellema and A. Frank, *Mon. Not. R. Astron. Soc.* **273**, 401 (1995); B. Balick, *Am. Sci.* **84**, 342 (1996).
13. A short description of the ROSAT satellite and its capabilities is given in *Sky Telesc.* **90**, 35 (August 1995).
14. According to recent results obtained by D. Pequinot (in *Proc. Int. Astron. Union Symp.* **180**, in press), 30 elements can be traced in PNe.
15. J. H. Lutz, in (37), pp. 19–22.
16. L. H. Aller, *Physics of Thermal Gaseous Nebulae* (Astrophys. and Space Library 112, Reidel, Dordrecht, Netherlands, 1984), pp. 98 and 120.
17. K. M. Xilouris, J. Papamastorakis, E. Paleologou, Y. Terzian, *Astron. Astrophys.* **310**, 603 (1996); K. J. Borkowski, C. L. Sarazin, N. Soker, *Astrophys. J.* **360**, 173 (1990).
18. R. W. Tweedy and R. Napiwotzki, *Astron. J.* **108**, 978 (1994).
19. H. E. Bond, R. Ciardullo, L. K. Fullton, K. Schaefer, in *Proc. Int. Astron. Union Symp.* **180**, in press.
20. J. B. Kaler, *Annu. Rev. Astron. Astrophys.* **23**, 89 (1985).
21. R. H. Mendez, R. P. Kudritzki, A. Herrero, D. Husfeld, H. G. Groth, *Astron. Astrophys.* **190**, 113 (1988).
22. AP Cygni profile is an emission line with a blueshifted absorption component.
23. M. Perinotto, in (37), pp. 57–64.
24. K. Werner and U. Heber, *Astron. Astrophys.* **247**, 476 (1991); T. Rauch, J. Köppen, K. Werner, *ibid.* **286**, 543 (1994); R. Napiwotzki, thesis, Christian-Albrechts-Universität zu Kiel (1993).
25. K. Werner and T. Rauch, *Astron. Astrophys.* **284**, L5 (1994).

26. I. Iben Jr., J. B. Kaler, J. W. Truran, A. Renzini, *Astrophys. J.* **264**, 605 (1983).
27. Y. Sakurai, *Int. Astron. Union Circ.* **6325** (1996); *Int. Astron. Union Circ.* **6328** (1996).
28. H. W. Duerbeck and S. Benetti, *Astrophys. J.* **468**, L111 (1996); F. Kerber *et al.*, in *Proc. Int. Astron. Union Symp.* **180**, in press; F. Kerber, H. Gratl, M. Roth, *Int. Astron. Union Circ.* **6601** (1997).
29. H. E. Bond, J. W. Liebert, A. Renzini, M. G. Meakes, in *ST-EFC/StSci Workshop: Science with the HST*, P. Benvenuti and E. Schreier, Eds. (European Southern Observatory, Garching, Germany 1992), pp. 139–141.
30. A. M. van Genderen and A. Gautschi, *Astron. Astrophys.* **294**, 453 (1995).
31. I. Iben, in (37), pp. 587–596.
32. G. Jacoby and R. Ciardullo, in (37), pp. 503–513.
33. J. J. Feldmeier, R. Ciardullo, G. H. Jacoby, *Astrophys. J.* **461**, L25 (1996).
34. M. Arnaboldi, S. Beaulieu, M. Capaccioli, K. C. Freeman, P. J. Quinn, *ESO Workshop on Science with the VL7*, J. R. Walsh and I. J. Danziger, Eds. (Springer, Berlin, 1995), pp. 232–235.
35. P. J. Huggins, in (37), pp. 147–154.
36. C. R. O'Dell and K. D. Handron, *Astron. J.* **111**, 1630 (1996).
37. R. Weinberger and A. Acker, Eds., *Proc. Int. Astron. Union Symp.* **155** (1993).
38. The PNe images are courtesy of B. Balick and J. Alexander (University of Washington), A. Hajian (U.S. Naval Observatory), M. Perinotto (University of Florence), P. Patriarchi (Arcetri Observatory, Florence), Y. Terzian (Cornell University and NASA), and R. Sahai and J. Trauger (JPL—California Institute of Technology), in collaboration with the Wide Field—Planetary Camera 2 IDT and NASA.

Using Neutron Stars and Black Holes in X-ray Binaries to Probe Strong Gravitational Fields

Philip Kaaret and Eric C. Ford

Neutron stars and black holes can be studied by observation of the radiation produced as matter falls into their gravitational fields. X-ray binaries, which are systems consisting of a neutron star or black hole and a companion gaseous star, produce radiation in this manner. Recently, oscillations at frequencies near 1000 cycles per second have been detected from x-ray binaries. These oscillations are likely produced in regions of very strong gravitational fields within a few tens of kilometers of the compact star. The oscillations have been interpreted as evidence for the existence of an innermost stable orbit near a compact star, a key prediction of general relativity theory. The study of x-ray binaries has also advanced the search for definitive evidence of black holes. Recent developments in our understanding of accretion flows in x-ray binaries have provided evidence for the existence of event horizons in x-ray binaries thought to contain black holes.

Neutron stars and stellar-mass black holes are born in the deaths of gaseous stars, when exhaustion of the nuclear energy of a star causes it to collapse under the pull of gravity. Here we consider x-ray binaries, which are stellar binary systems composed of a black hole or neutron star in orbit with a companion gaseous star, in which the compact star is made visible by matter taken from the companion and drawn toward the compact star (1). Matter falling in the gravitational field of the compact star gains kinetic energy that can be released as radiation. In certain x-ray binaries, x-ray emission can arise from a region only a few tens of kilometers across near the compact star. These x-rays are a direct probe of the region of strong gravitational fields near the compact star.

Perhaps the strongest motivation for the study of x-ray binaries is to investigate

strong gravitational fields. Because the radius of a stellar-mass neutron star is only about 10 km, the gravitational field at the surface of a neutron star is 10^5 times stronger than at the surface of the sun. In gravitational fields of such strength, qualitatively distinct predictions arise when general relativity is compared to Newtonian theories of gravity. One such prediction of general relativity is that matter orbiting sufficiently close to a compact star will be unable to maintain a stable orbit and will fall into the star (2). A possible signature of the boundary between stable and unstable orbits has been identified in oscillations detected from neutron star x-ray binaries during the past year (3).

Observations of x-ray binaries may also provide evidence of objects that have suffered complete gravitational collapse: black holes (4). The most striking difference between a black hole and a neutron star is that neutron stars have surfaces whereas black holes do not. The boundary of a black

The authors are at the Columbia Astrophysics Laboratory, Columbia University, New York, NY 10027, USA. E-mail for P. Kaaret: kaaret@astro.columbia.edu